



WEDNESDAY SLIDE CONFERENCE 2013-2014

Conference 23

23 April 2014

---

**CASE I:** 10N-1078 (JPC 4002848).

**Signalment:** Adult gravid female koi, (*Cyprinus carpio koi*).

**History:** The adult female koi was submitted to UC Davis, VMTH Companion Avian and Exotic Animal Medicine and Surgery/Aquatic Animal

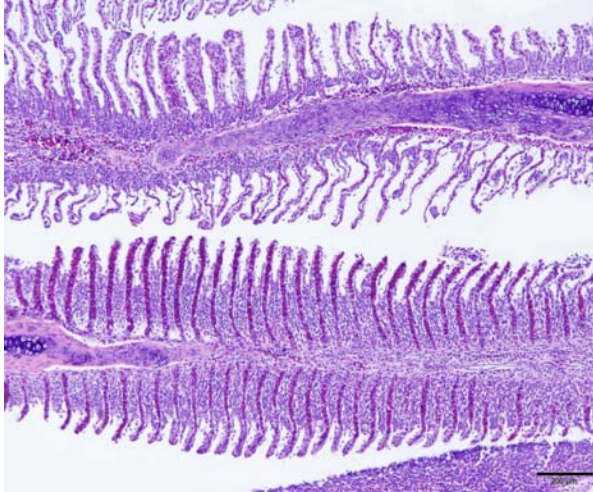
Health service, dead on arrival from a non-commercial pond. Three other koi had died over the past 10-month period (August 2009 through May 2010), with similar clinical signs. The owner reported that this fish developed ulcerations on the dorsal head a few months ago and had been lethargic for the past three to four days. After being isolated from the pond, it



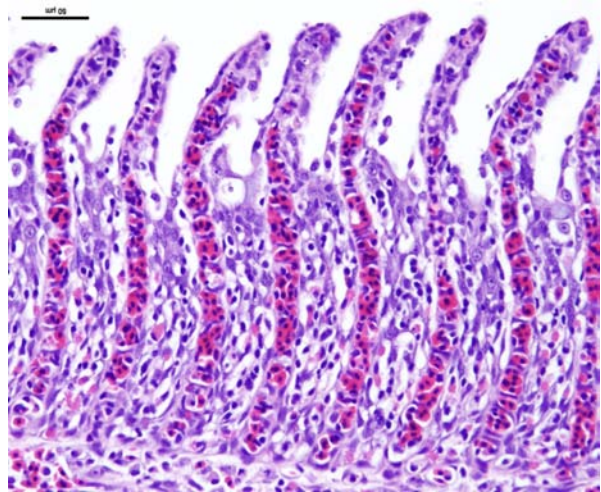
1-1. Skin, koi: There was an irregular, coalescing, well demarcated area of scale and skin loss with exposed underlying subcutis and muscles at the dorso-lateral trunk. The eroded areas were surrounded with hemorrhage. (Photo courtesy of: UC Davis School of Veterinary Medicine, Anatomic Pathology Department, One Shields Ave, Davis, CA 95616 <http://www.vetmed.ucdavis.edu/pmi/>)



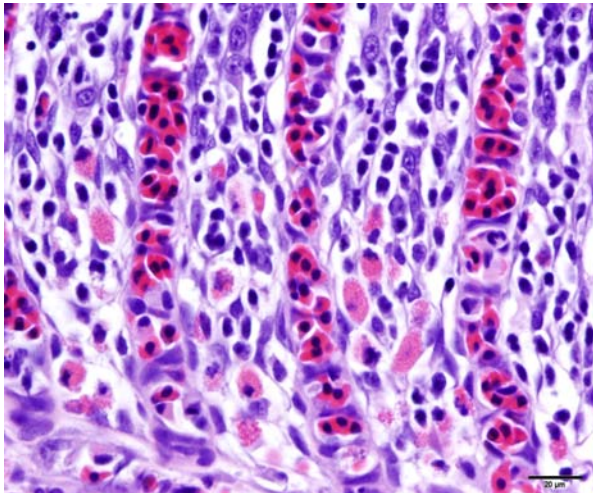
1-2. Skin around vent, koi: Diffusely throughout the body, clear fluid was exuding from the vesicles expanding the skin and elevating the scales producing a "pinecone" appearance. Pink discolorations of the skin as shown around the vent were due to petechiae and small congested vessels. (Photo courtesy of: UC Davis School of Veterinary Medicine, Anatomic Pathology Department, One Shields Ave, Davis, CA 95616 <http://www.vetmed.ucdavis.edu/pmi/>)



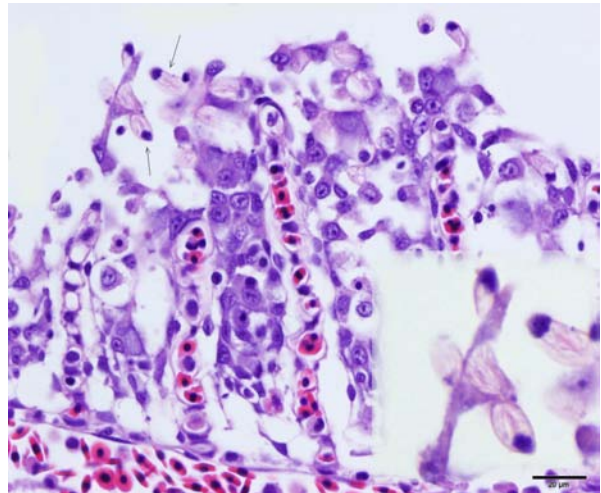
1-3. Gill, koi: Low power view demonstrates clubbing and fusion of the gill lamellae. Interstitial edema, necrosis and detachment of gill epithelium are also present. (HE 40X) (Photo courtesy of: UC Davis School of Veterinary Medicine, Anatomic Pathology Department, One Shields Ave, Davis, CA 95616 <http://www.vetmed.ucdavis.edu/pmi/>)



1-4. Gill, koi: Low power view demonstrates clubbing and fusion of the gill lamellae. Interstitial edema, necrosis and detachment of gill epithelium are also present. (HE 40X) (Photo courtesy of: UC Davis School of Veterinary Medicine, Anatomic Pathology Department, One Shields Ave, Davis, CA 95616 <http://www.vetmed.ucdavis.edu/pmi/>)



1-5. Gill, koi: Gill inflammation consists of mononuclear cells and granular leukocytes. (HE 400X) (Photo courtesy of: UC Davis School of Veterinary Medicine, Anatomic Pathology Department, One Shields Ave, Davis, CA 95616 <http://www.vetmed.ucdavis.edu/pmi/>)



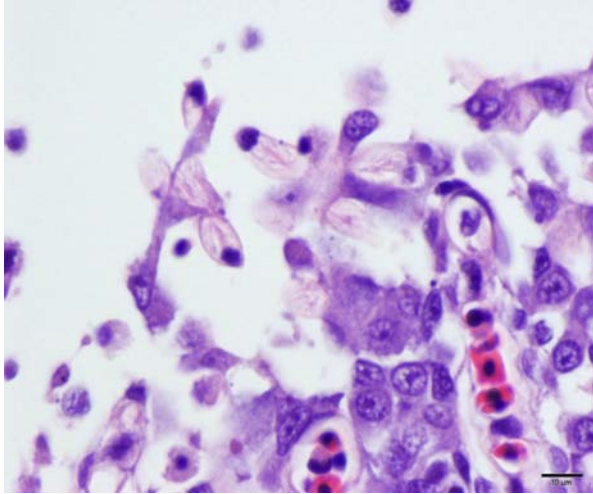
1-6. Gill, koi: High magnification of gill secondary lamellae demonstrates gill epithelium degeneration, necrosis and numerous rodlet cells. (HE 400X) (Photo courtesy of: UC Davis School of Veterinary Medicine, Anatomic Pathology Department, One Shields Ave, Davis, CA 95616 <http://www.vetmed.ucdavis.edu/pmi/>)

developed generalized edema. The other affected fish similarly developed ulcerations prior to death. The owner offered antibiotic-containing feed to the pond after the third fish died. The pond is a converted swimming pool also being used by waterfowl.

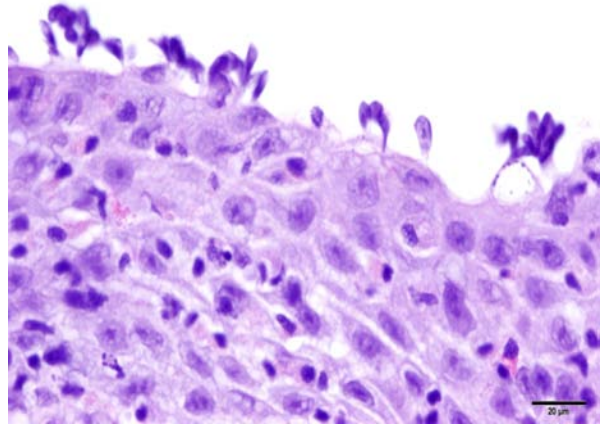
Upon clinical examination, ulceration on the lateral trunk and prominent edema of the gills were noted. Post mortem gill biopsy and skin scrapings were done using light microscopy immediately on arrival, and revealed gill flukes

(*Dactylogyrus* sp.). Skin scraping did not reveal additional findings.

The fish was submitted for full necropsy to rule out viral, including koi herpes virus (KHV, Cyprinid herpesvirus 3), spring viremia of carp virus (SVCV), or bacterial infections. Fresh samples of gill and kidney were tested for KHV and carp edema virus (CEV). The molecular techniques used were PCR as described by Oyamatsu T. et al., for CEV and Taqman - PCR for KHV by Bercovier H. et al. A sample of



1-7. Gill, koi: Closer view of the rodlet cells. (HE 600X) (Photo courtesy of: UC Davis School of Veterinary Medicine, Anatomic Pathology Department, One Shields Ave, Davis, CA 95616 <http://www.vetmed.ucdavis.edu/pmi/>)



1-8. Skin, koi: Adjacent to the ulcerated regions, on the intact epidermal surface, there were thin pyriform protozoa attached by thin stalks (flagella), approximately 6x5 mm (similar in size to a red blood cell), consistent with *Ichthyobodo* sp., (formerly known as *Costia* sp.). (HE 400X) (Photo courtesy of: UC Davis School of Veterinary Medicine, Anatomic Pathology Department, One Shields Ave, Davis, CA 95616 <http://www.vetmed.ucdavis.edu/pmi/>)

water from the pond was submitted for toxicological and other water quality analyses.

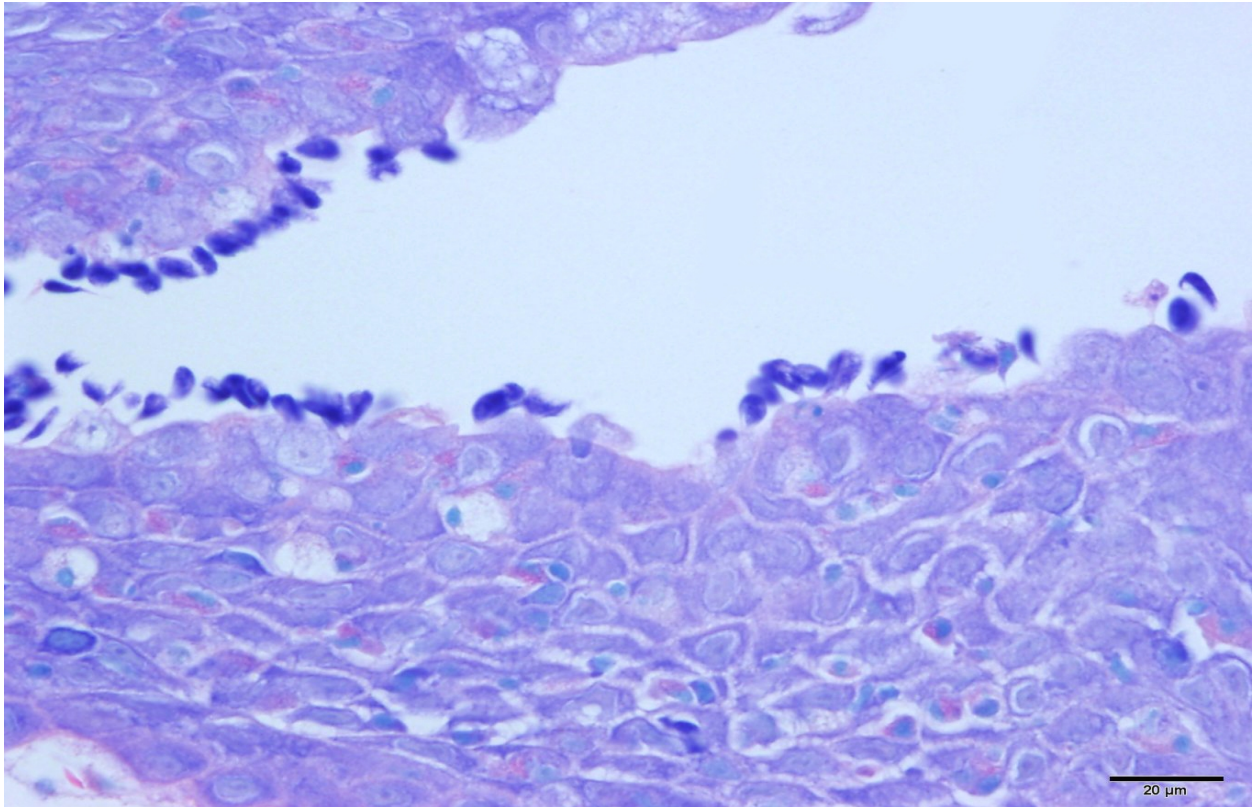
**Gross Pathology:** The submitted fish had irregular, coalescing, well demarcated areas of scale and skin loss with exposed underlying subcutis and muscles at the dorso-lateral trunk. The eroded areas were surrounded with hemorrhage. Diffusely, the scales fell out with little manipulation of the body. Clear fluid was exuding from the vesicles expanding the skin and elevating the scales producing a “pinecone” appearance. The skin on the head, around the vent, and diffusely throughout the body, had numerous pinpoint red discolorations (consistent with petechiation) and small vessel congestion. The mucosa of the upper palate of the mouth was diffusely swollen, partially occluding the pharyngeal region. The coelomic organs were intertwined and adhered to the parietal serosa with numerous thin fibrous attachments. The ovary, liver, spleen and kidneys were extremely friable. The gastrointestinal tract was surrounded with a large amount of adipose tissue.

**Laboratory Results:**

- Molecular analysis of the fresh tissues (gill, kidney) were positive for Carp Edema Virus (CEV) or “Koi Sleepy Disease,” a pox - like virus, and negative for KHV.

- Toxicological analysis of the water did not demonstrate any elevated heavy metals except for copper, measuring 0.02ppm (reference at 0.01ppm).
- Elevated nitrite (0.085mg/L NO<sub>2</sub>-N) and ammonia nitrogen (0.11mg/L NH<sub>3</sub>-N) were detected using spectrophotometer.

**Histopathologic Description:** Gill: The secondary gill lamellae are partially fused due to marked, diffuse epithelial cell hyperplasia and hypertrophy, mixed interstitial inflammation and edema. The interstitium of the primary lamellae is also expanded with marked edema and contains mixed inflammation. The inflammation consists of abundant mononuclear cells, such as lymphocytes and macrophages, as well as eosinophilic granular cells. Thickened and distorted secondary lamellae are lined with plump, sometimes vacuolated epithelium that piles up into confluent sheets with admixed inflammation, particularly at the base of the filaments. The gill epithelial cells frequently have rounded margins, hypereosinophilic cytoplasm, and karyorrhectic, pyknotic or indistinct nuclei. Sloughed necrotic cells mix in with cellular debris and erythrocytes at the gill surface. There is rare multifocal rodlet cell hyperplasia throughout the affected regions. Rare gill arch arterioles contain fibrin thrombi. Multifocally in the gill and mucosal epithelium, smudged basophilic aggregates and sometimes eosinophilic material



1-9. Skin, koi: Pyriiform protozoa attached to the intact epidermal surface adjacent to the ulcer are highlighted with Giemsa. (Giemsa, 400X) (Photo courtesy of: UC Davis School of Veterinary Medicine, Anatomic Pathology Department, One Shields Ave, Davis, CA 95616 <http://www.vetmed.ucdavis.edu/pmi/>)

disperses the chromatin (presumed cytoplasmic invagination, early chromatin changes in necrotic cells). Vessels throughout the gill are dilated.

Skin (slide not provided): Associated with superficial areas of ulceration are small, gram-negative bacterial aggregates (presumed *Aeromonas* sp.) mixed in with rare gram-positive larger rods. Adjacent to the ulcerated regions, on the intact epidermal surface, there were thin pyriform protozoa attached by thin stalks (flagella), approximately 6x5 μm (similar in size to a red blood cell), consistent with *Ichthyobodo* sp., (formerly known as *Costia* sp.). The scales are elevated above the dermis by clear spaces (edema). Skeletal muscles in the region of skin ulceration are inflamed and necrotic. The myocytes have fragmented, vacuolated or pale eosinophilic sarcoplasm with loss of distinct striations. Mononuclear inflammatory, often fragmented cells aggregate between myocytes, and along with erythrocytes spill onto the exposed surface.

- Contributor's Morphologic Diagnosis:**
1. Gill: Moderate diffuse subacute necrotizing branchitis with marked interstitial edema and multifocal branchial arteriole thrombosis (PCR positive for carp edema virus).
  2. Integument, mid left dorso-lateral body wall: Severe multifocal subacute regionally extensive ulcerative and fibrinohemorrhagic dermatitis and necrotizing myositis with epidermal protozoal parasites (probable *Ichthyobodo* sp.).
  3. Integument: Severe diffuse edema, petechiation, scale loss and lymphocytic and granulocytic dermatitis.

**Contributor's Comment:** Carp edema virus (CEV) is the causative agent of sleepy disease of koi (SDK) with devastating outbreaks in koi or ornamental variety of carp (*Cyprinus carpio koi*, also known as Japanese color carp). This disease occurs epizootically in the fall and spring in commercially cultured young fish. Occurrence of outbreaks is associated with mild water temperature ranges of 15 to 25 degrees Celsius. Affected fish are lethargic, found at the bottom/surface of the tank or pond with sunken eyes and

skin erosions/ulcerations. The most distinct gross finding is diffuse edema, particularly affecting the gills. Microscopic findings include clubbing and swelling of gill filaments with interlamellar fusion, and hypertrophy, hyperplasia and necrosis of the gill epithelium. CEV, a pox – like virus, particles can be visualized with transmission electron microscopy in the infected gill epithelium.<sup>6</sup> Electron microscopy demonstrates cytoplasmic viral particles in the gill epithelium with immature virus measuring up to 450nm in diameter and mature, roughly oval, virions measuring about 400x413nm. Mature virions are decorated with surface globules and have a dense core enclosed by a prominent membrane.<sup>6</sup> Cytoplasmic inclusions characteristic of pox virus infections were not observed in the gills of this fish, neither they were described by T. Miyazaki et al. The CEV PCR assay can detect the virus in multiple different tissues from affected fish including skin, liver and kidney.<sup>6</sup>

In this case, the diagnosis of carp edema virus was made on the characteristic gross and histologic findings with confirmation by PCR. No virions were identified in gill tissue by electron microscopy; however, the tissue was not optimally preserved. Combination of CEV, protozoal, and bacterial infections may have played a role in the skin ulceration. The latter two could potentially be opportunistic pathogens infecting the compromised host.

Based on the history (mild water temperature, season, age of affected fish) and gross lesions (skin ulcerations and petechiae), differentials for this case would include KHV and SVC. The pronounced branchial edema distinguishes the CEV infection, grossly. As a brief review, KHV is characterized grossly by necrotizing branchitis and is a reportable disease of wild and cultured common carp. Histological findings include epithelial proliferation, fusion of the gill lamellae, and epithelial necrosis (cytopathic effect of the virus). Typical of KHV, there are intranuclear inclusions in many cell types, including but not limited to respiratory epithelial cells, macrophages, hematopoietic cells in the kidney, and cardiac myocytes. Electron microscopy demonstrates enveloped herpes virus with mature nucleocapsids measuring up to 117nm and mature enveloped nucleocapsids up to 180nm in the affected cells.<sup>7</sup> KHV virus can be isolated from multiple organs and confirmed with PCR and

immunohistochemistry.<sup>2,5</sup> Spring viremia of carp virus (SVCV) from the family Rhabdoviridae, genus *Vesiculovirus*, is the causative agent of another reportable, contagious, fatal disease of farmed carp and related species. The virus causes petechial hemorrhages in the gill and skin, as well as internal hemorrhage in the kidneys, spleen and liver, and exophthalmia. SVCV targets the swim bladder, resulting in edema and inflammation, as well as ascites.<sup>1,3</sup> Skin ulceration can also be caused by parasitic infection such as *Ichthyobodo* sp. (formerly known as *Costia* sp.) that may also affect the gills.<sup>4,9</sup> The latter agent can be seen on scrapings from gills and skin lesions, and on histological examination. Koi ulcer disease (also known as summer ulcer disease and carp erythrodermatitis), associated with bacterial pathogens such as *Aeromonas* spp., can also present similarly.<sup>4,9</sup>

**JPC Diagnosis:** 1. Gill: Branchitis, proliferative, diffuse, severe, with marked epithelial hypertrophy and hyperplasia, lamellar fusion, arteriolar fibrin thrombi and mild goblet cell hyperplasia.  
2. Oral mucosa: Stomatitis, proliferative and lymphocytic, diffuse, mild, with numerous intraepithelial intranuclear inclusions.

**Conference Comment:** The moderator began with a brief review of the normal anatomy, histology and physiology of the gill. The gill arch is a curved bony structure with double rows of paired primary lamellae (filaments). Each primary lamella, in turn, encompasses an array of perpendicularly oriented secondary lamellae. The entire gill arch is covered by epidermis; the epidermis overlying the origin of the primary lamellae is thicker and often contains numerous mucous cells, with a subepidermal array of lymphoid tissue. The primary lamellae are covered by a mucoid epidermis which may contain round, pale, eosinophilic, salt-secreting chloride cells (especially at the basal/proximal part of the lamellae). These chloride cells function in ionic transport and may also play a role in detoxification.<sup>8</sup>

Gas exchange occurs via countercurrent exchange at the surface of the secondary lamellae, which are lined by overlapping squamous epithelial cells, usually one layer thick, surrounding numerous capillaries that are supported by rows of pillar cells. Where the pillar cells encroach on

the basement membrane, they spread to coalesce with neighboring pillar cells to complete the lining of lamellar blood channels. Pillar cells contain contractile protein elements that resist distension and support the lamellar blood spaces. The surface of the lamellar epithelium gives rise to microvilli that aid in attachment of the epidermal (cuticular) mucus. This mucus, in addition to providing protection against abrasion and infection, is important in the exchange of gas, water and ions. The combined thickness of the cuticle, respiratory epithelium and flanges of the pillar cells (which is the total diffusion distance for gas exchange) ranges from 0.5 to 4  $\mu\text{m}$ . Low to moderate numbers of goblet cells are scattered among lamellar squamous epithelial cells of both primary and secondary lamellae.<sup>8</sup>

Much like mammalian lungs, the gill epithelium is thin with a large surface area in order to maximize the exposure of gill capillaries to water. While this is an important factor for efficient gas exchange, it is a fairly ineffective physical barrier and results in increased branchial vulnerability to inflammation and infection. Gills also play an essential role in regulating the exchange of salt and water, as well as the excretion of the nitrogenous wastes (primarily ammonia). Thus, even minimal damage can result in significant osmoregulatory and respiratory difficulties.<sup>8</sup>

As noted by the contributor, the proliferative nature of these microscopic lesions is striking, with marked epithelial cell hypertrophy and hyperplasia leading to lamellar fusion; however, many conference participants also identified moderate numbers of fairly prominent, eosinophilic, intracytoplasmic inclusions within the epithelium of the (presumed) oral mucosa, which appear to peripheralize the chromatin. After scrupulous examination of H&E sections, and consideration of the laboratory results reported by the contributor (molecular analysis for koi herpes virus was negative), we are unable to elucidate the nature of these inclusions. There is also some slide variation - not all sections contain fibrin thrombi within arterioles of the gill arch, as reflected in the JPC morphologic diagnosis. Furthermore, the moderator observed that cartilage of the gill arch appears somewhat irregular and deformed, which may suggest a previous nutritional deficiency, but is probably unrelated to the current disease process.

**Contributing Institution:** UC Davis School of Veterinary Medicine  
Anatomic Pathology Department  
One Shields Ave  
Davis, CA 95616  
<http://www.vetmed.ucdavis.edu/pmi/>

**References:**

1. Ahne W, Bjorklund HV, Essbauer S, et al. Spring viremia of carp (SVC). *Dis of Aquat Org.* 2002;52:261–272.
2. Bercovier H, Fishman Y, Nahary R, et al. Cloning of the koi herpesvirus (KHV) gene encoding thymidine kinase and its use for a highly sensitive PCR based diagnosis. *BMC Microbiol.* 2005;5:13.
3. Dikkeboom AL, Radi C, Toohey-Kurth K, et al. First report of spring viremia of carp virus (SVCV) in wild common carp in North America. *Journal of Aquatic Animal Health.* 2004;16:169–178.
4. Ferguson HW. *Systemic Pathology of Fish.* 2nd ed. London, UK: Scotian Press; 2006:55, 72-73.
5. Ilouze M, Dishon A, Kotler M. Characterization of a novel virus causing a lethal disease in carp and koi. *Microbiology and Molecular Biology Reviews.* 2006;70:147–156.
6. Miyazaki T, Isshiki T, Katsuyuki H. Histopathological and electron microscopy studies on sleepy disease of koi (*Cyprinus carpio koi*) in Japan. *Dis of Aquat Org.* 2005;65:197–207.
7. Miyazaki T, Kuzuya Y, Yasumoto S, et al. Histopathological and ultrastructural features of koi herpesvirus (KHV)-infected carp *Cyprinus carpio*, and the morphology and morphogenesis of KHV. *Dis of Aquat Org.* 2008;80:1–11.
8. Mumford S, Heidel J, Smith C, Morrison J, MacConnell B, Blazer V. *Fish Histology and Histopathology.* US Fish and Wildlife Service, National Conservation Training Center. <http://nctc.fws.gov/resources/course-resources/fish-histology/index.html>. Accessed April 26, 2014.
9. Noga EJ. *Fish Disease: Diagnosis and Treatment.* St. Louis, MO: Wiley-Blackwell; 1996:108-110, 141-146.

**CASE II: 10-5509 (JPC 4006285).**

**Signalment:** Adult male zebrafish, (*Danio rerio*).

**History:** This fish was submitted as part of a breeding pair being screened for infection by *Pseudoloma neurophilia* prior to placing their bleached embryos on the system. Fish were processed by making a ventral midline incision to facilitate fixation and placing in Bouin's solution for 24 hours. The entire fish was then bisected parasagittally, and four levels were taken at 100  $\mu$ m increments for histopathologic evaluation. Each level was stained with both H&E and Luna stain to screen for *Pseudoloma*.

**Gross Pathology:** None.

**Histopathologic Description:** Within the brainstem and spinal cord, few microsporidian xenomas are present that range in size from approximately 20-40  $\mu$ m in diameter, and which contain aggregates of ovoid spores measuring approximately 5.5 x 2.5  $\mu$ m. The spores are uninucleate and are segregated into sporophorous vesicles within the xenoma. A few developmental stages (sporoblasts) are also present within the xenomas. Additionally, several nerve roots contain individual spores, either free or within the cytoplasm of macrophages. Individual spores are best visualized on the Luna-stained section, in which they stain dark orange. The neuropil adjacent to the xenomas is free of an

inflammatory response. A mild histiocytic response is present within the nerve roots in association with individual spores.

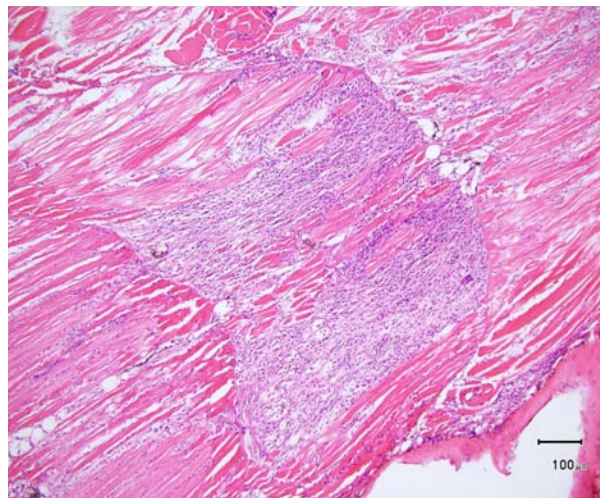
**Contributor's Morphologic Diagnosis:** 1. Brain, spinal cord: Microsporidian xenomas, few, morphology consistent with *Pseudoloma neurophilia*.  
2. Nerve roots: Radiculoneuritis, histiocytic, multifocal, mild, with intralesional microsporidian spores (morphology consistent with *Pseudoloma neurophilia*).

**Contributor's Comment:** *Pseudoloma neurophilia* is a microsporidian parasite related to *Loma* and *Ichthyosporidium*, which also infect fish and lead to the formation of xenomas within various tissues.<sup>5</sup> It is reported to be the most common pathogen in zebrafish facilities.<sup>3</sup> Mild infections (as was present in this case) may be associated with no clinical signs; however, heavily infected fish (which we have also encountered in our laboratory) often demonstrate significant weight loss (known as "skinny disease") and/or scoliosis. Fish with mild to moderate infections have been shown to exhibit poor growth and reproductive performance, particularly in the face of other environmental stressors.<sup>7</sup>

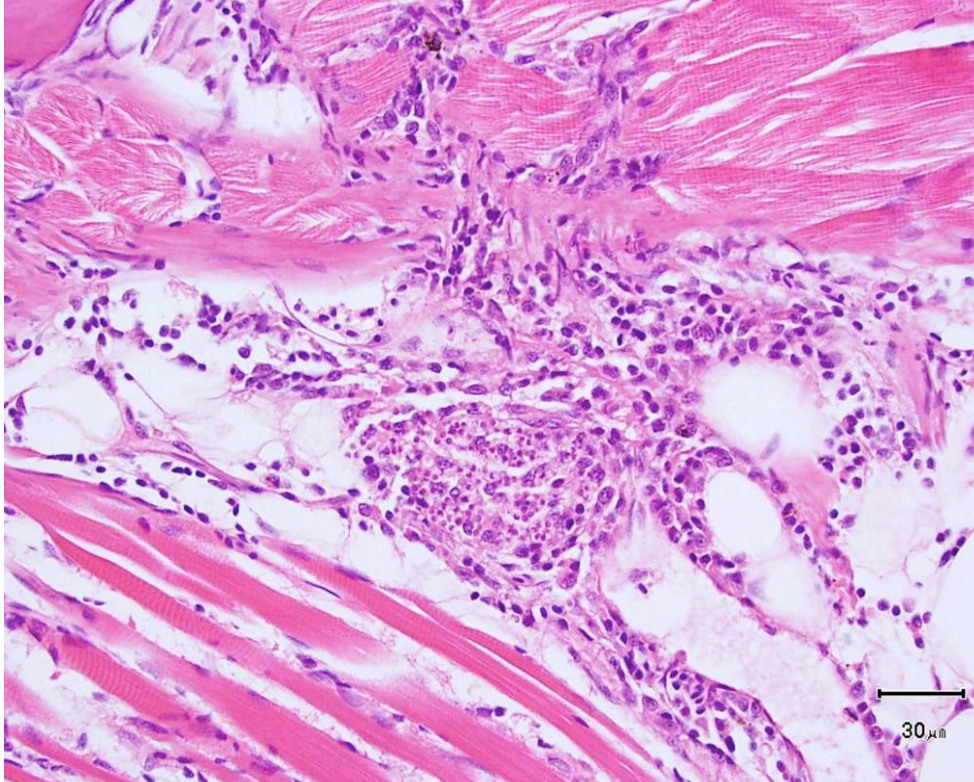
Xenomas, which may measure up to 200  $\mu$ m in diameter, are composed of several aggregates of up to 16 uninucleate spores segregated within



2-1. Zebrafish, presentation: This individual presented with poor weight gain and scoliosis. (Photo courtesy of: Laboratory of Comparative Pathology, Memorial Sloan Kettering Cancer Center, New York, NY 10065 <http://www.mskcc.org>)



2-2. Zebrafish, skeletal muscle: Multifocally, skeletal muscle is infiltrated by large numbers of macrophages and exhibits moderate to severe myodegeneration and atrophy. (Photo courtesy of: Laboratory of Comparative Pathology, Memorial Sloan Kettering Cancer Center, New York, NY 10065 <http://www.mskcc.org>)



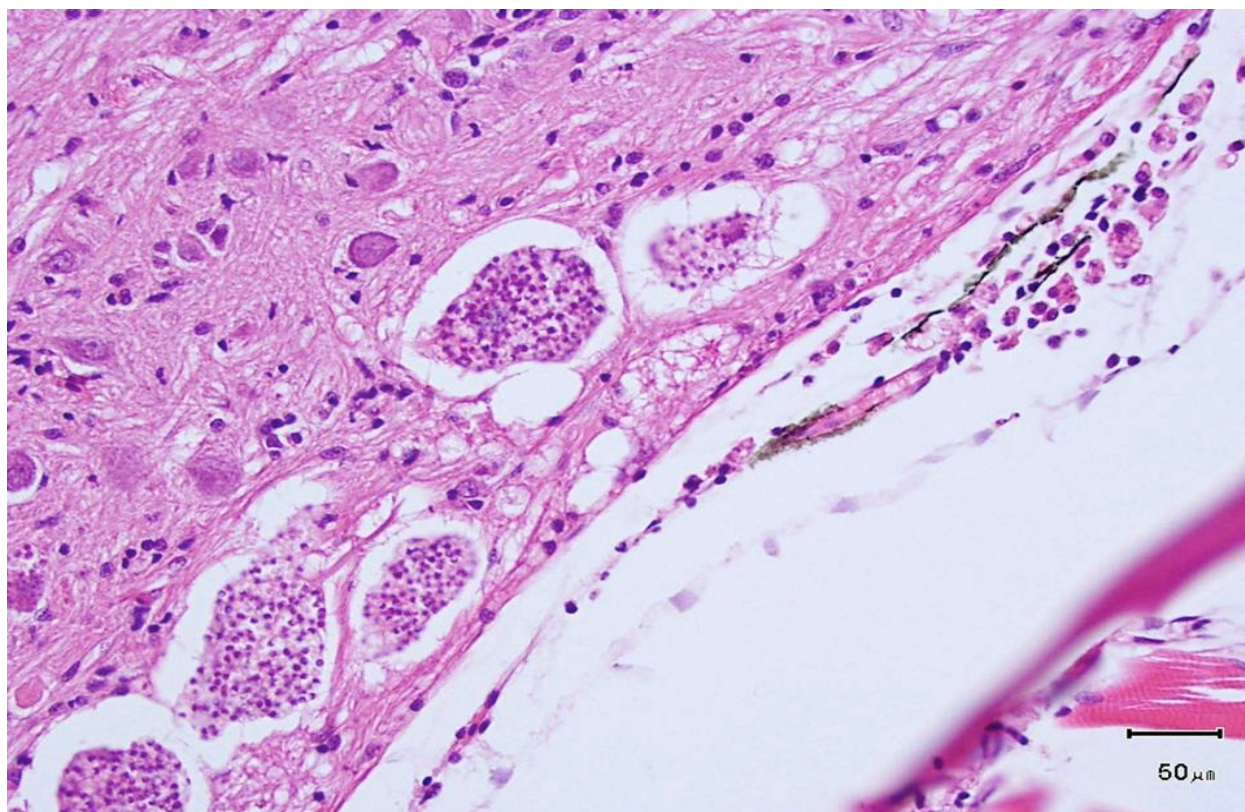
2-3. Zebrafish, skeletal muscle: Scattered throughout inflammatory foci are low numbers of myxosporidian cysts which, when rupture, are surrounded by numerous macrophages, which often contain phagocytosed spores. (HE 400X) (Photo courtesy of: Laboratory of Comparative Pathology, Memorial Sloan Kettering Cancer Center, New York, NY 10065 <http://www.mskcc.org>)

sporophorous vesicles. Spores are oval to pyriform and measure approximately 5.5 x 2.5  $\mu\text{m}$ . Like other microsporidians, the spores contain a polar filament. In addition to mature spores, sporophorous vesicles contain a few developmental stages known as sporoblasts. Unlike many other microsporidia, developmental stages are in direct contact with the host cytoplasm, rather than within parasitophorous vacuoles, based on electron microscopic studies.<sup>5</sup>

As was the case in this fish, a few xenomas usually do not stimulate a significant inflammatory response; however, large numbers of xenomas and/or the presence of free spores within tissues may be associated with significant inflammation. In heavily infected fish, the inflammatory reaction may extend from the spinal cord meninges or nerve roots into the adjacent skeletal musculature, where it may be associated with massive chronic inflammation and myodegeneration, with relatively few organisms present (either within xenomas or free spores which undergo phagocytosis by macrophages).

Transmission is primarily through the ingestion of infective spores, either free in the water or within the tissues of cannibalized fish. Experimental transmission following exposure of fish to water contaminated with organisms derived from infected spinal cords resulted in infection as early as 8 weeks post-exposure, with 100% of exposed fish infected by week 20.<sup>4</sup> As its name implies, *P. neurophilia* has a tendency to infect the central nervous system (particularly the brainstem and spinal cord), as well

as nerve roots. However, both xenomas and free spores have been identified in other tissues, particularly the ovary and developing follicles, leading to speculation that vertical transmission (or at least transmission via sexual products released during spawning) may occur. Because of this and the fact that routine chlorine bleaching does not appear to kill the infective spores,<sup>1</sup> techniques involving re-derivation of colonies by the screening of adult fish using histopathology and/or of a percentage of their offspring by PCR have been developed and are being used by some facilities (including ours) in order to create SPF lines.<sup>3</sup> In addition to being used to test adults and eggs, PCR may be used to test water filtrates, biofilms, and other samples.<sup>8</sup> Histopathologic diagnosis is greatly facilitated by the use of a Luna stain, which binds to chitin and stains spores bright orange.<sup>6</sup> Other histochemical stains, such as Gram, Fite's acid-fast, and Giemsa are variably effective in staining spores. Spores may also be visualized using fluorescent stains (Fungi-Fluor).<sup>4</sup> No treatment is currently available,<sup>3</sup> and infections persist following exposure, with no evidence for immune clearance by the host.<sup>7</sup>



2-4. Zebrafish, spinal cord: Low to moderate numbers of intact xenomas are scattered throughout the spinal cord. (HE 400X) (Photo courtesy of Laboratory of Comparative Pathology, Memorial Sloan Kettering Cancer Center, New York, NY 10065 <http://www.mskcc.org>)

**JPC Diagnosis:**

1. Brain: Microsporidial xenomas, multiple.
2. Spinal cord: Ganglioneuritis, histiocytic, multifocal, mild, with intracytoplasmic microsporidian spores.

**Conference Comment:** The contributor provides an excellent summary of *Pseudoloma neurophilia* infection in fish; readers are urged to review WSC 2013-2014, conference 4, case 3 for a detailed discussion of other microsporidian species encountered in veterinary medicine. Microsporidia are obligate intracellular, unicellular eukaryotes that are most closely related to fungi, specifically zygomycetes. They have one of the smallest known genomes and exist extracellularly only as small, thick-walled spores with a coiled polar filament. Developing spores can be packaged within a parasitophorous vacuole (e.g., *Encephalitozoon* spp.) or can remain within the cytoplasm (e.g., *Enterocytozoon bieneusi*, *Nosema* spp.).<sup>2</sup> Interestingly, the conference moderator notes that some microsporidia (including *P. neurophilia*) appear birefringent under polarized light.

**Contributing Institution:** Laboratory of Comparative Pathology  
 Memorial Sloan Kettering Cancer Center  
 New York, NY 10065  
<http://www.mskcc.org>

**References:**

1. Ferguson JA, Watral V, Schwindt AR, Kent ML. Spores of two fish microsporidia (*Pseudoloma neurophilia* and *Glugea anomala*) are highly resistant to chlorine. *Dis Aquat Org.* 2007;76:205-214.
2. Keeling PJ, McFadden GI. Origins of microsporidia. *Trends Microbiol.* 1998;6(1):19-23.
3. Kent ML, Buchner C, Watral VG, Sanders JL, LaDu J, Peterson TS, Tanguay RL. Development and maintenance of a specific pathogen-free (SPF) zebrafish research facility for *Pseudoloma neurophilia*. *Dis Aquat Org.* 2011;95:73-79.
4. Kent ML, Bishop-Stewart JK. Transmission and tissue distribution of *Pseudoloma neurophilia* (Microsporidia) of zebrafish, *Danio rerio* (Hamilton). *J Fish Dis.* 2003;26:423-426.
5. Matthews JL, Brown AMV, Larson K, Bishop-Stewart JK, Rogers P, Kent ML. *Pseudoloma*

*neurophilia* n. g., n. sp., a new microsporidian from the central nervous system of the zebrafish (*Danio rerio*). *J Eukaryot Microbiol.* 2001;48:227-233.

6. Peterson TS, Spitsbergen JM, Feist SW, Kent ML. Luna stain, an improved selective stain for detection of microsporidian spores in histologic sections. *Dis Aquat Org.* 2011;95:175-180.

7. Ramsay JM, Watral V, Schreck CB, Kent ML. *Pseudoloma neurophilia* infections in zebrafish *Danio Rerio*: effects of stress on survival, growth, and reproduction. *Dis Aquat Org.* 2009;88:69-84.

8. Whipps CM, Kent ML. Polymerase chain reaction detection of *Pseudoloma neurophilia*, a common microsporidian of zebrafish (*Danio rerio*) reared in research laboratories. *J Am Assoc Lab Ani Sci.* 2006;45:13-16.

**CASE III:** U-30918-12 (JPC 4032588).

**Signalment:** Mature adult unknown gender Atlantic Salmon, (*Salmo salar*).

**History:** These fish are from a research facility where they are held in 1500L tanks at approximately 12°C, pH of ~8, nitrogen gas saturation ~100 % and oxygen at 80 % saturation. Tissues were collected during end of study post-mortem examinations on extra salmon. The study duration was no greater than 24 months.

**Gross Pathology:** The right pseudobranch was swollen and mottled.

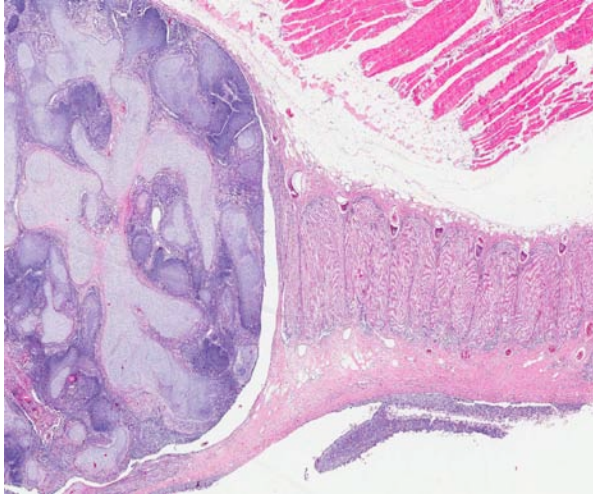
**Histopathologic Description:** Expanding and effacing the pseudobranch is a non-encapsulated, well demarcated, expansile, highly cellular mass composed of three haphazardly intermingled cellular populations embedded in small amounts of dense fibrous stroma. These cell populations consist of dense aggregates of basophilic blastemal cells, polygonal to cuboidal epithelial cells and islands of cartilage. Epithelial populations often consist of cuboidal cells which

sometimes form structures resembling branchial lamellae. In other areas, dense cords and trabeculae of epithelial cells often are intermingled with numerous round cells with small dense, eccentrically located nuclei which are compressed against the cell margins by moderate amounts of pink, round cytoplasm (interpreted as mucous producing goblet cells). Blastemal cells are round to slightly spindloid, darkly basophilic and have sparse, poorly defined, cytoplasm, round to ovoid, dark nuclei with finely stippled chromatin and unapparent to small, nucleoli. Islands of cartilage are often surrounded by concentric layers of thin spindloid cells with scant, poorly defined, pale basophilic cytoplasm, fusiform, nuclei with finely stippled chromatin and unapparent nucleoli. The mitotic rate is 10 figures noted in ten randomly selected fields at high power objective (40x) with mitotic figures only observed within the epithelial populations. Multifocal aggregates of lymphocytes and granular leucocytes are present at the periphery of the mass.

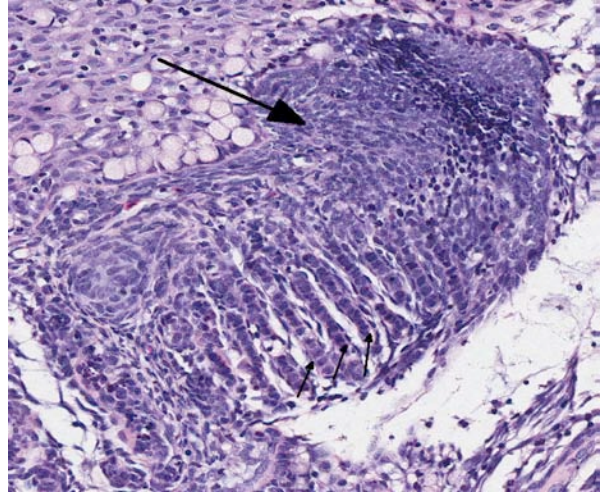
**Contributor's Morphologic Diagnosis:**  
Pseudobranch: Branchioblastoma.



3-1. Pseudobranch, salmon: An 8mmx6mm well-demarcated expansile neoplasm expands the pseudobranch. (HE 0.63X)



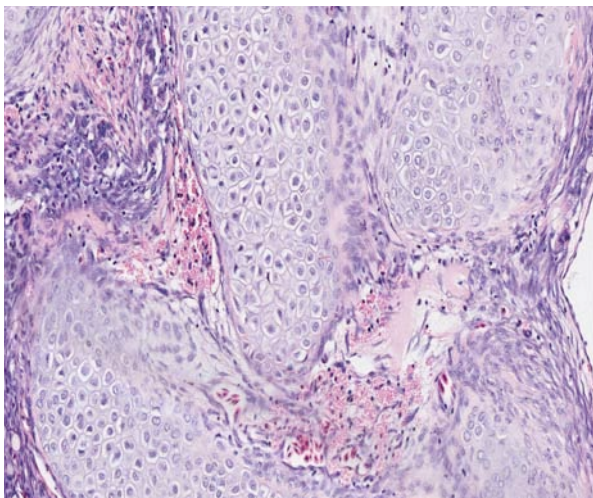
3-2. Pseudobranch, salmon: The neoplasm is composed of multiple lobules of small, densely packed blastemal cells separated by thick trabeculae of well-differentiated cartilage. These components are similar to those seen in the pseudobranch, but markedly disordered. (HE 14X)



3-3. Pseudobranch, salmon: Densely packed polygonal to spindle blastemal cells (large arrow), occasionally are arranged into structures resembling secondary lamellae. (HE 164X)

**Contributor's Comment:** There is increasing interest in the use of fish as models for carcinogenicity studies as well as ecosystem monitors within the environment.<sup>6,7</sup> Neoplasms of the gill and pseudobranch are rare compared to other locations such as the skin or liver, but have been previously described in koi carp (*Cyprinus carpio*).<sup>3</sup> To the author's knowledge, it has not been previously reported in Atlantic salmon (*Salmo salar*).

Branchioblastoma is a tumor of embryologic blast-type cells with mesenchymal and epithelial components. It is histologically considered a benign tumor because it is expansile and often



3-4. Pseudobranch, salmon: Scattered among cartilage trabeculae and nests of blastemal cells are large numbers of granulated leukocytes. (HE 220X)

well demarcated. However, the mass can interfere with gaseous exchange in the gill with potentially fatal consequences. Affected fish may present with respiratory distress, an inability to close their mouth or multilobulated mass/masses appearing to originate from a gill arch or the pseudobranch.<sup>3</sup>

Select differentials for a multilobular lesion in the region of the operculum, gill and oral cavity may include granulomatous or inflammatory lesions due to infection by bacteria (eg. *Mycobacterium* sp.), fungi (eg. *Banichiomyces*), microsporidia (eg. *Loma* sp.), myxozoa (eg. *Myxobolus* sp.), branchial trematodes, and iridovirus (eg. lymphocystis).

Neoplasia in fish is likely multifactorial and has previously been associated with exposure to carcinogens,<sup>6</sup> genetic causes,<sup>5</sup> and retrovirus infection.<sup>1</sup> No underlying cause was identified in this case.

**JPC Diagnosis:** Pseudobranch: Branchioblastoma.

**Conference Comment:** The pseudobranch is not found in all fish species, but where present it is a red, gill-like tissue attached to the internal surface of the operculum. It is composed of cartilage-supported parallel blood capillaries that create a counter-current system which likely functions to increase oxygen uptake. The pseudobranch has a direct vascular connection with the ocular choroid, which is composed of similar capillary

arrays alternating with rows of slender fibroblast-like cells; it may also play a role in the filling of the air bladder.<sup>4</sup>

In addition to branchioblastoma, which can arise from the gill or the pseudobranch and may be spontaneous or carcinogen-induced,<sup>3</sup> conference participants briefly discussed teratoma as a rule-out with similar histological features. Branchioblastoma, as noted by the contributor, is composed of embryologic blast-type cells with mesenchymal and epithelial components; similarly, teratomas are classically defined as having at least two of the three embryonic layers—endoderm, mesoderm, and ectoderm (see WSC 2013-2014, conference 8, case 2). Teratomas occur most frequently in the gonads; however, these tumors can also develop at extragonadal locations, usually along the midline.<sup>2</sup> They are rarely (if ever) reported in fish. The moderator points out that branchioblastoma and teratoma have analogous etiopathogeneses; however, the neoplastic cell types comprising branchioblastomas are appropriate to the anatomic location (i.e. this tumor appears to be attempting to form normal gill tissue in a relatively normal location), while teratomas tend to produce poorly differentiated, disorganized tissue that does not belong (i.e. foci of squamous epithelium, bone and tooth within the gonad). Based on these broad attributes, this neoplasm is most consistent with a branchioblastoma.

**Contributing Institution:** Department of Pathology/Microbiology  
Atlantic Veterinary College  
University of Prince Edward Island  
550 University Avenue  
Charlottetown, Prince Edward Island  
C1A 4P3  
<http://avc.upei.ca/diagnosticservices>

**References:**

1. Coffee L, Casey J, Bowser P. Pathology of tumors in fish associated with retroviruses: a review. *Vet Pathol.* 2013;50:390-403.
2. Foster RA. Male reproductive system. In: McGavin MD, Zachary JF, eds. *Pathologic Basis of Veterinary Disease*. 5th ed. St. Louis, MO: Elsevier; 2012:1142-1143.
3. Knüsel R, Brandes R, Lechleiter S, Schmidt-Posthaus H. Two independent cases of spontaneously occurring branchioblastomas in koi

- carp (*Cyprinus carpio*). *Vet Pathol.* 2007;44:237-239.
4. Mumford S, Heidel J, Smith C, Morrison J, MacConnell B, Blazer V. *Fish Histology and Histopathology*. US Fish and Wildlife Service, National Conservation Training Center. <http://nctc.fws.gov/resources/course-resources/fish-histology/index.html>. Accessed April 26, 2014.
5. Shin J, Padmanabhan A, de Groh E, Lee J-S, Haidar S, Dahlberg S, et al. Zebrafish neurofibromatosis type 1 genes have redundant functions in tumorigenesis and embryonic development. *Dis Model Mechan.* 2012;5:881-894.
6. Williams D, Bailey G, Reddy A, Hendricks J, Oganessian A, Orner G, et al. The rainbow trout (*Oncorhynchus mykiss*) tumor model: recent applications in low-dose exposures to tumor initiators and promoters. *Toxicol Pathol.* 2003;31:58-61.
7. Wirgin I, Waldman J. Altered gene expression and genetic damage in North American fish populations. *Mutation Res.* 1998;399:193-219.

**CASE IV:** 65066 (JPC 4032696).

**Signalment:** 20-year-old male white-lipped mud turtle, (*Kinosternon leucostomum*).

**History:** This turtle was from a large regional aquarium collection and presented to veterinary clinicians with coelomic distension and periocular swelling. Ultrasound examination confirmed coelomic effusion that was classified as a transudate following fluid analysis. Radiographs demonstrated diffuse, bilateral mineral opacities within the kidneys. Bloodwork showed a moderate anemia and severe elevation in uric acid. With a presumptive diagnosis of chronic renal failure in an elderly and fractious turtle, the animal was maintained on hospice care without further diagnostics. The turtle died 3.5 months after initial presentation.

**Gross Pathology:** Grossly, there was severe coelomic distention and subcutaneous edema of the neck and limbs. Both kidneys were diffusely off-white and hard, with no normal renal tissue



4-1. Radiograph, dorsoventral view, white-lipped mud turtle: The kidneys are outlined by diffuse bilateral mineral opacities. (Photo courtesy of: Johns Hopkins University School of Medicine, Dept. of Molecular and Comparative Pathobiology, <http://www.hopkinsmedicine.org/mcp/>)

apparent. The liver was friable and enlarged with rounded edges and multifocal green-tan mottling.

**Histopathologic Description:** Approximately 80% of the renal parenchyma is replaced by anastomosing trabeculae of well-differentiated mature bone. The bone contains scattered osteocytes and the trabecular surface is lined by flattened to cuboidal osteoblasts and occasional multinucleated osteoclasts. In non-ossified parenchyma, there is moderate, multifocal expansion of the interstitium by increased clear space (edema) and loosely arranged, fusiform to stellate cells (fibroblasts), as well as scattered infiltrates of mixed inflammatory cells including lymphocytes, plasma cells, heterophils, and azurophils. Remaining renal tubules are frequently ectatic, and/or lined by variably enlarged epithelial cells with abundant indistinct cytoplasmic vacuolization (hydropic degeneration). Increased cytoplasmic basophilia and occasional mitotic figures are also observed among tubular epithelial cells, suggestive of tubular regeneration. Flocculent, lightly eosinophilic proteinaceous material is often present within tubular lumens along with rare cellular debris. Glomeruli are multifocally affected by mild segmental thickening of the mesangial matrix and capillaries by lightly eosinophilic material and mild hypercellularity (membranoproliferative glomerulonephritis).

**Contributor's Morphologic Diagnosis:** Kidneys, nephropathy, diffuse, chronic, severe, with marked osseous metaplasia, fibroplasia, tubular degeneration, mild membranoproliferative glomerulonephritis, mild lymphocytic and granulocytic interstitial nephritis.

**Contributor's Comment:** Osseous metaplasia (ectopic ossification), the formation of non-neoplastic bone in soft tissues, has been reported to occur in numerous extra-skeletal organ systems and in the setting of many, clinically disparate disease processes. The ectopic osseous matrix can be mineralized and is typically associated with osteocytes, osteoclasts, osteoblasts, and, in some cases, hematopoietic cells and adipocytes. It is frequently encountered in veterinary medicine as an incidental lesion in the pulmonary connective tissue of dogs and cattle and in the canine dura mater (ossifying pachymeningitis). Ectopic ossification has also been reported in a

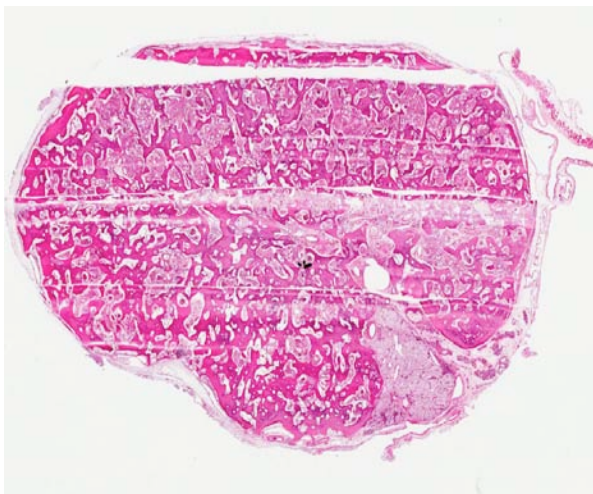


4-2. Radiograph, lateral view, white-lipped mud turtle: The kidneys are outlined by diffuse bilateral mineral opacities. (Photo courtesy of: Johns Hopkins University School of Medicine, Dept. of Molecular and Comparative Pathobiology, <http://www.hopkinsmedicine.org/mcp/>)

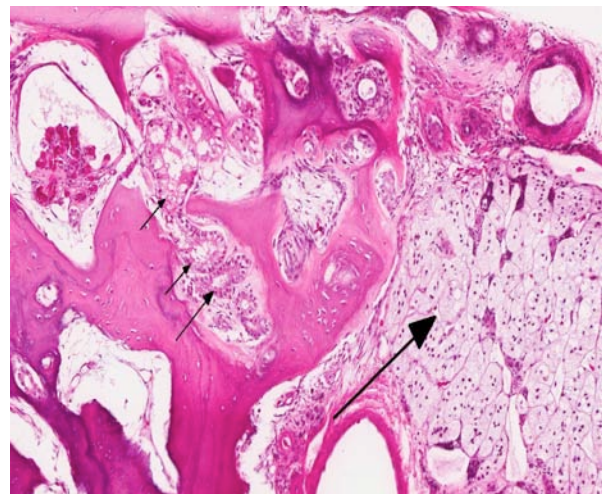
spectrum of human and animal neoplasms, notably in canine mammary tumors, where it is a common feature.<sup>1</sup> For reasons that are not entirely clear, non-mammalian species empirically are more prone to developing osseous metaplasia than mammals.

Ectopic bone either arises from embryonic cell rests or by differentiation of adult, pluripotent mesenchymal cells into osteoblasts (osseous

metaplasia).<sup>2</sup> Osseous metaplasia can occur anywhere uncommitted mesenchymal cells reside, including skeletal muscle, perivascular tissue, and connective tissue or sites of tissue regeneration and repair. It requires the influence of local osteogenic signals in an environment conducive to bone production.<sup>3</sup> Chronic ischemia, trauma, persistent hematoma, chronic inflammation, neoplasia, hypercalcemia, and hypervitaminosis D are among the factors known to stimulate osseous



4-3. Kidney and adrenal gland, white-lipped mud turtle: The kidneys are largely replaced by trabeculae of lamellar bone. (HE 0.63X)



4-4. Kidney and adrenal gland, white-lipped mud turtle: The kidneys are largely replaced by trabeculae of lamellar bone. Glomeruli, tubules (small arrows) and adrenal gland are encased within bony trabeculae. (HE 130X)

metaplasia.<sup>4,5</sup> While the pathophysiologic mechanisms leading to bone formation is not completely understood, paracrine signaling leading to the expression of bone morphogenetic proteins (BMPs) is likely a common key factor.<sup>3</sup> Most BMPs are members of the TGF beta superfamily and are critical signaling agents in normal development and differentiation and in the formation of new bone during fracture healing.<sup>6</sup> BMP expression has been demonstrated to play a role in neoplastic processes associated with ectopic bone formation, as well as experimental models of chronic inflammation.<sup>7</sup> In addition to non-committed mesenchymal cells, vascular endothelial cells<sup>8</sup> and pericytes<sup>9</sup> have also been implicated as potential cells of origin for osseous metaplasia. Interestingly, inactivating germline mutations of the  $\alpha$ -subunit of the stimulatory G protein gene leads to subcutaneous and sometimes deeper ectopic bone formation in humans (Albright hereditary osteodystrophy) and in mice.<sup>10</sup> Osseous metaplasia is also seen in association with dystrophic cardiac and pulmonary mineralization in particular strains of mice where early events involve abnormal cellular calcium, mitochondrial alterations, and myocyte injury in the absence of elevation of serum calcium.<sup>12,13</sup>

While pathologic mineralization within the kidney is a not an uncommon finding in cases of chronic renal disease, the presence of abundant, trabecular bone in the renal parenchyma of this turtle is remarkable. Reports of spontaneous osseous metaplasia in the kidney are rare in the human medical literature and even rarer in the veterinary medical literature. In humans, ossified tissue in the kidney is associated with chronic interstitial nephritis, chronic ischemia, pyelonephritis, and papillary necrosis, and it is an uncommon nidus for renal calculus formation.<sup>5,11</sup> Contributing factors for renal osseous metaplasia observed in this turtle likely included chronic inflammatory stimulation and possibly calcium/phosphorous imbalance secondary to chronic renal dysfunction.

**JPC Diagnosis:** 1. Kidney: Osseous metaplasia, diffuse, severe, with renal tubular degeneration and necrosis.  
2. Kidney: Nephritis, interstitial, lymphoplasmacytic, diffuse, moderate.

**Conference Comment:** We thank the contributor for providing such a thorough summary of

osseous metaplasia in veterinary species, and we concur with the proposed explanation that a combination of mineral imbalance due to chronic renal dysfunction (supported by the clinical pathology results and radiographs) and chronic inflammatory stimulation likely contributed to the striking pathologic findings observed in this case. Conference participants briefly considered osteoma as a rule out; however, this benign tumor is generally attached to the periosteum and should not result in the incorporation of renal glomeruli/tubules within bony trabeculae. Additionally, the moderator observed that some tissue sections contain portions of adrenal gland adjacent to the renal hilus, which is a normal anatomic location in some turtle species. Conference participants also noted that the large collecting duct within the hilus appears to contain numerous spermatozoa.

**Contributing Institution:** Johns Hopkins University School of Medicine  
Dept. of Molecular and Comparative Pathobiology  
<http://www.hopkinsmedicine.org/mcp/>

#### References:

1. Thompson K. Bones and joints. In: Maxie MG, ed. *Jubb, Kennedy, and Palmer's Pathology of Domestic Animals*. Vol. 1. 5th ed. Philadelphia, PA: Saunders Elsevier, 2007:1-184.
2. Myers R, McGavin M, Zachary J. Cellular adaptations, injury, and death: morphologic, biochemical, and genetic basis. In: Zachary JF, McGavin MD, eds. *Pathologic Basis of Veterinary Disease*. 5th ed. St. Louis, MO: Elsevier; 2012:2-59.
3. McCarthy EF, Sundaram M. Heterotopic ossification: a review. *Skeletal Radiol*. 2005;34:609-619.
4. Landim FM, Tavares JM, de Melo Braga DN, da Silva JE, Bastos Filho JBB, Feitosa RGF. Vaginal osseous metaplasia. *Arch Gynecol Obstet*. 2009;279:381-384.
5. Bataille S, Daniel L, Legris T, Vacher-Coponat H, Purgus R, Berland Y, Moal V. Osseous metaplasia in a kidney allograft. *Nephrol Dial Transplant*. 2010;25:3796-3798.
6. Wozney JM, Rosen V. Bone morphogenetic protein and bone morphogenetic protein gene family in bone formation and repair. *Clin Orthop Relat Res*. 1998;346:26-37.
7. Rifas L. T-cell cytokine induction of BMP-2 regulates human mesenchymal stromal cell

- differentiation and mineralization. *J Cell Biochem.* 2006;98:706–714.
8. Medici D, Olsen BR. The role of endothelial-mesenchymal transition in heterotopic ossification. *J Bone Miner Res.* 2012;27:1619–1622.
9. Dayoub S, Devlin H, Sloan P. Evidence for the formation of metaplastic bone from pericytes in calcifying fibroblastic granuloma. *J Oral Path Med.* 2003;32:232–236.
10. Huso DL, Edie S, Levine MA, Schindinger W, Wang Y, Harald J, Germain-Lee EL. Heterotopic Ossifications in a mouse model of Albright hereditary osteodystrophy. *Plos One.* 2011;6:e21755.
11. Fernandez-Conde M, Serrano S, Alcover J, Aaron JE. Bone metaplasia of urothelial mucosa: an unusual biological phenomenon causing kidney stones. *Bone.* 1996;18:289–291.
12. Percy DH, Barthold SW. *Pathology of Laboratory Rodents and Rabbits.* 3rd ed. Ames, IA: Iowa State Press; 2007:94-95, 219.
13. Ernst H, Dungworth DL, Kamino K, Rittinghausen S, Mohr U. Nonneoplastic lesions in the lungs. In: Mohr U, Dungworth DL, Capen CC, Carlton WW, Sundberg JP, Ward JM, eds. *Pathobiology of the Aging Mouse.* Washington, DC: ILSI Press; 1996:298.